

# AUTONOMOUS DRUG DESIGN WITH MULTI-ARMED BANDITS

Hampus Gummesson Svensson<sup>\*,1,2</sup>, Esben Bjerrum<sup>†,2</sup>, Christian Tyrchan<sup>3</sup>, Ola Engkvist<sup>1,2</sup>, and Morteza Haghir Chehreghani<sup>1</sup>

<sup>1</sup>Chalmers University of Technology, Department of Computer Science and Engineering, Gothenburg, Sweden

<sup>2</sup>AstraZeneca, Molecular AI, Discovery Sciences, BioPharmaceuticals R&D, Gothenburg, Sweden

<sup>3</sup>AstraZeneca, Medicinal Chemistry, Research and Early Development, Respiratory and Immunology (R&I), BioPharmaceuticals R&D, Gothenburg, Sweden

## ABSTRACT

Recent developments in artificial intelligence and automation could potentially enable a new drug design paradigm: autonomous drug design. Under this paradigm, generative models provide suggestions on thousands of molecules with specific properties. However, since only a limited number of molecules can be synthesized and tested, an obvious challenge is how to efficiently select these. We formulate this task as a contextual stochastic multi-armed bandit problem with multiple plays and volatile arms. Then, to solve it, we extend previous work on multi-armed bandits to reflect this setting, and compare our solution with random sampling, greedy selection and decaying-epsilon-greedy selection. To investigate how the different selection strategies affect the cumulative reward and the diversity of the selections, we simulate the drug design process. According to the simulation results, our approach has the potential for better exploring and exploiting the chemical space for autonomous drug design.

**Keywords** Drug Design · Multi-armed Bandits · Sequential Decision-making

## 1 Introduction

Developing a new drug is a complex process that can take up to a decade and cost more than US \$1 billion [17]. A crucial part of this process is to design novel clinical drug candidates with desired molecular properties [8]. Drug candidates are usually identified in an iterative optimization process consisting of four steps, the so-called Design-Make-Test-Analyze (DMTA) cycle. In the design step, molecules are designed to have some specific properties, including a high binding affinity to a specific protein. In the make step, it is decided how to synthesize them. After being synthesized, the properties of the molecules are experimentally measured in the test step. Subsequently, in the analyze step the newly gathered experimental data is used to improve the design choices in the next round.

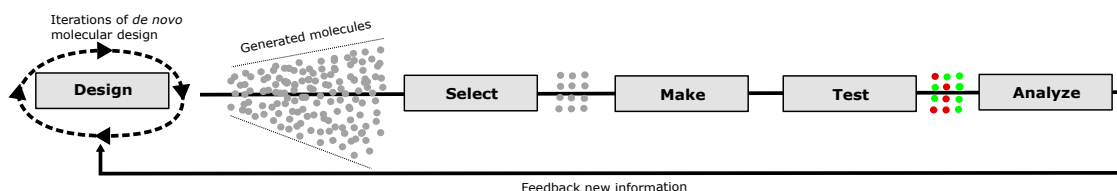


Figure 1: A schematic illustration of the drug design process, including the selection that must be made in the autonomous drug design paradigm.

\*Corresponding author: hamsven@chalmers.se

†This author is currently at Odyssey Therapeutics, Cambridge, MA, USA.

Two new paradigms have emerged to increase the productivity in drug design: *de novo* molecular design and accelerating the DMTA cycle through automation. Recent advances in *de novo* molecular design utilize generative models for sampling the chemical space and in this way generate molecules with specific desirable properties [11]. The automation of the DMTA cycle takes advantage of automated laboratories and machine learning to make, test and analyze molecules with minimal human intervention [4, 5, 7, 16]. Taken together, this progress can lead to *autonomous drug design*. Under such paradigm, *de novo* molecular design is used to generate an extensive list of molecules using limited prior information. However, it is only possible to make a fraction of the molecules, as illustrated in Figure 1, since each experiment is both costly and time-consuming. Even if it would be possible to synthesize all generated molecules, it can be more efficient to obtain new information sequentially.

This work is focused on how to select molecules to make in order to explore and exploit the chemical space efficiently. In each iteration, we obtain a list of molecules that can be selected. In theory, there are approximately  $10^{60}$  molecules that are in the total set of selectable molecules [14]. Each molecule has a context in terms of descriptor(s) that encodes its features, e.g., the Morgan fingerprint [12], a popular way to encode structural features of molecules in a bit or count vector. Moreover, when utilizing *de novo* molecular design to suggest promising molecules, the selectable set can be different in each iteration, which makes it even more challenging. Compared to other works that have focused solely on *de novo* molecular design [1] or automating the synthesis of molecules [3], we simulate all steps of the DMTA cycle by creating a digital twin. Previous work by Matveieva and Polishchuk [10] has shown that predictive models trained on structural features of molecules are able to learn ground truths determined by pre-defined patterns, e.g., number of nitrogen. Given a ground truth that simulates the test scores of a desired target, this enables us to investigate how the choices in one cycle affect the following cycles.

We study this problem in the context of multi-armed bandits (MAB), where the goal is to adaptively compute the most informative decisions. Considering the problem at hand, we regard the following characteristics of the MAB problem: (1) base arms are volatile, meaning that in each round, new arms may arrive; (2) the expected outcome of a base arm depends on its context; (3) multiple base arms are played in each iteration; (4) the set of context-arm pairs is infinite. To solve this problem adequately, we propose to extend the contextual Zooming algorithm [15] to our setting. This in contrast to Chen et al. [2] who utilizes a fixed hypercube partition of the context space and Nika et al. [13] who adaptively creates a tree partition. We use the available structural contexts, which together with Jaccard distance provides a natural similarity space, to adaptively create a partition of the context space. To the best of our knowledge, this is the first study that simulates an automated DMTA cycle and in this context investigates a multi-armed bandits approach to determine which molecules to make next.

## 2 Problem Formulation

We formulate the drug design task as a stochastic multi-armed bandits problem proceeding over  $T$  rounds by extending the work of Nika et al. [13] and Slivkins [15] to adapt to the specifications of our task. Each base arm is defined by its  $D$ -dimensional context  $x$ , belonging to the context space  $\mathcal{X} \subseteq \mathbb{R}^D$ . Moreover, for each pair of base arms with contexts  $x, x' \in \mathcal{X}$ , we have a similarity distance  $0 \leq \mathcal{D}_{\mathcal{X}}(x, x') \leq 1$  that measures the dissimilarity between them. The context space and similarity distance create a similarity space  $(\mathcal{X}, \mathcal{D}_{\mathcal{X}})$ . In our problem, arms are molecules, the contexts are molecular fingerprints and the similarity distance measures the chemical dissimilarity. The outcome of a base arm with context  $x$  is denoted by  $R(x)$ , which is a Bernoulli random variable that takes values in  $\{0, 1\}$ . We assume that there exists an unknown function  $\mu(x) : \mathcal{X} \rightarrow \{0, 1\}$  such that  $\mu(x) = \mathbb{E}[R(x)]$ ,  $\forall x \in \mathcal{X}$ . This unknown function is determined by a ground truth that simulates our desired target.

At round  $t$ , a set of  $M^t > K$  base arms, indexed by the set  $\mathcal{M}^t$ , arrive with contexts  $\mathcal{X}^t$  and scores  $\mathcal{F}^t$  such that  $x_m^t$  is the context of base arm  $m \in \mathcal{M}^t$  in round  $t$ . The score  $f_m^t$  of a base arm  $x_m^t$  is the estimated probability of  $\mu(x_m^t) > 0.5$ , i.e.,  $x_m^t$  corresponds to an active molecule. This score is given by a machine learning model, which we hereafter call the scoring function, that has been trained on previous observations. After the base arms, contexts and scores have been observed, a selection strategy is used to select a super arm  $\mathcal{S}^t \subset \mathcal{M}^t$  of  $K$  base arms. Next, for each base arm  $m \in \mathcal{S}^t$ , a reward  $r(x_m^t)$  is observed. The objectives are to maximize the cumulative reward by round  $T$  and find a diverse set of base arms with high rewards. This corresponds to finding a set of *novel* drug candidates by round  $T$ .

## 3 Contextual Zooming with multiple plays and volatile arms

In this section, we introduce our approach, contextual Zooming with multiple plays and volatile arms, summarized in Algorithm 1. It is an extension of the contextual Zooming algorithm [15] to our task. In addition, we use the *doubling trick* to incrementally increase the time horizon  $T$  but, for the sake of brevity, this is not included in the algorithm description.

---

**Algorithm 1:** Contextual zooming with multiple plays and volatile arms.

---

**Input:** Similarity space  $(\mathcal{X}, \mathcal{D}_{\mathcal{X}})$  of diameter  $\leq 1$ **Data:** Collection of initial history  $\mathcal{H}_0$  consisting of plays of initial base arms and corresponding rewards.**Init:**  $B \leftarrow B(p, 1)$ ; Add initial history  $\mathcal{H}_0$  to  $B$ ;  $\mathcal{A} \leftarrow B$ 

```

1 for each round  $t = 1, \dots, T$  do
2   Observe base arms in  $\mathcal{M}^t$  and their contexts  $\mathcal{X}^t$ 
3    $\mathcal{R}^t \leftarrow \{B \in \mathcal{A} : \exists m \in \mathcal{M}^t, m \in \text{dom}(B, \mathcal{A})\}$ 
4   Compute indices  $g^t(B), \forall B \in \mathcal{R}^t$ 
5   Compute indices  $g^t(x_m^t), \forall m \in \mathcal{M}^t$ 
6    $\mathcal{S}^t \leftarrow \text{Oracle}(g^t(x_1^t), \dots, g^t(x_{M^t}^t))$ 
7    $\mathcal{C}^t \leftarrow \{B \in \mathcal{R}^t : \exists m \in \mathcal{S}^t, m \in \text{dom}(B, \mathcal{A})\}$ 
8   Observe reward  $r(x_m^t)$  for each base arm  $m \in \mathcal{S}^t$ 
   // Update counters for each ball
9   for  $m \in \mathcal{S}^t$  do
10     $n(B_m^t) \leftarrow n(B_m^t) + 1$ 
11     $\text{rew}(B_m^t) \leftarrow \text{rew}(B_m^t) + r(x_m^t)$ 
12  for  $B \in \mathcal{C}^t$  do
13    if  $\text{conf}(B) \leq \text{radius}(B)$  then
14       $x'_t \leftarrow \max\{x_m^t : m \in \mathcal{S}^t, \mathcal{C}_m^t = B\}$ 
15       $B' \leftarrow B(x'_t, \frac{1}{2}\text{radius}(B))$ 
16      Update  $n(B')$  and  $\text{rew}(B')$  by adding relevant history
17       $\mathcal{A} \leftarrow \mathcal{A} \cup \{B'\}$ 

```

---

In each round  $t$ , there is a set of activated balls  $\mathcal{A}$ , where each ball  $B \in \mathcal{A}$  constitutes a ball with radius  $\text{radius}(B)$  in the similarity space. After base arms  $\mathcal{M}^t$  and contexts  $\mathcal{X}^t$  have been observed, the set of relevant balls  $\mathcal{R}^t$  is determined. A ball  $B \in \mathcal{A}_t$  is relevant if its *domain* covers at least one of the base arms in  $\mathcal{M}^t$ . The *domain* of ball  $B$  is a subset of  $B$  that excludes all balls  $B' \in \mathcal{A}_t$  with smaller radius  $\text{radius}(B')$

$$\text{dom}_t(B) \triangleq B \setminus \left( \bigcup_{B' \in \mathcal{A}_t : \text{radius}(B') < \text{radius}(B)} B' \right).$$

For each relevant ball  $B \in \mathcal{R}^t$ , we calculate its index as defined by Slivkins [15]

$$g^t(B) \triangleq \text{radius}(B) + \min_{B' \in \mathcal{A}_t} (I_t^{\text{pre}}(B') + \mathcal{D}(B, B')),$$

where  $\mathcal{D}(B, B')$  is the dissimilarity between the centers of the two balls. The *pre-index*  $I_t^{\text{pre}}$  of ball  $B$  is defined by

$$I_t^{\text{pre}}(B) \triangleq \nu_t(B) + \text{radius}(B) + \text{conf}_t(B),$$

where  $\nu_t(B) \triangleq \frac{\text{rew}_t(B)}{\max(1, n_t(B))}$  is the average reward of ball  $B$ , given by the total reward  $\text{rew}_t(B)$  and total number of plays

$n_t(B)$  of ball  $B$ . Moreover,  $\text{conf}_t(B)$  is the confidence radius of ball  $B$  at time  $t$ , given by  $\text{conf}_t(B) \triangleq 4\sqrt{\frac{\log T}{1+n_t(B)}}$ .

Given the indices of all relevant balls, we want to compute indices of all base arms in  $\mathcal{M}^t$ . We investigate two methods to determine the indices of the base arms. The first method computes the indices by

$$g^t(x_m^t) = f_m^t g^t(B_m^t), \forall m \in \mathcal{M}^t,$$

where  $B_m^t \in \mathcal{R}^t$  is the (relevant) ball covering base arm  $m$ . We call this method weighted contextual Zooming with multiple plays and volatile arms (weighted Zooming in short). The second method computes the indices by

$$g^t(x_m^t) = g^t(B_m^t), \forall m \in \mathcal{M}^t.$$

We call this variant unweighted contextual Zooming with multiple plays and volatile arms (unweighted Zooming in short). Given the indices of each base arm, we want to select a super arm  $\mathcal{S}^t$  of  $K$  base arms. This is done using an oracle that selects the set of  $K$  base arms with the largest cumulative index and breaks ties arbitrarily, as illustrated in Algorithm 2. Given the observed rewards for each base arm in  $\mathcal{S}^t$ , we refine the partition if the confidence radius of a ball  $B$  is less than or equal to its radius. Then, we create a new ball  $B'$  with half the radius of  $B$ . The center of  $B'$  is the base arm with the largest reward that was selected in the current round and is covered by ball  $B$ . For new ball  $B'$ , we add all relevant history from  $B$ , meaning that we update the counters using the previously observed base arms in the *domain* of  $B'$ . Lastly, we add the new ball  $B'$  to the set of activated balls  $\mathcal{A}$ .

**Algorithm 2:** Oracle

---

```

1 def Oracle( $g_1, \dots, g_M$ ):
2    $\mathcal{S} \leftarrow \max_{C \subseteq \{1, \dots, M\}: |C|=K} \sum_{i \in C} g_i$ 
3   return  $\mathcal{S}$ 

```

---

## 4 Experiments

We investigate different strategies that in each round  $t$  select a super arm  $S^T$  of molecules (base arms). For each selection strategy, we perform 10 runs, where each run corresponds to 200 sequential cycles of a simulated DMTA cycle or in other words  $T = 200$  rounds of the stochastic multi-armed bandits problem formulated in Section 2. As context for each base arm, we use the 2048-bit Morgan fingerprints [12] with radius 2 and counts of structural features generated utilizing RDKit [9]. To measure the dissimilarity between two contexts, we use the Jaccard distance. Below, we describe the simulated DMTA cycle, additional selection strategies and demonstrate the corresponding results.

### 4.1 Simulation of an DMTA cycle

**Design** We use the *de novo* molecular design tool REINVENT [1] to generate chemical molecules. In each iteration of REINVENT, 128 molecules are generated and, subsequently, scored by the scoring function. The score of each molecule is the probability of a positive outcome (active molecule). To improve the generation, each score is fed into the learning loop without any transformation. REINVENT performs at least 500 iterations of generation. If the highest score, over all previous iterations, is not improved over 50 iterations in a row, REINVENT stops. Moreover, REINVENT is used with the identical Murcko scaffold diversity filter with a bucket size of 100, minimum score of 0.2 and minimum similarity of 0.6.

As scoring function, we use a quantitative structure-activity relationship (QSAR) model based on a random forest model. The initial QSAR model is trained on 20 active and 100 inactive molecules, with respect to the ground truth, that were randomly sampled from ChEMBL [6] using REINVENT. The QSAR model is retrained in each iteration of the analyze step to learn the newly acquired data.

**Make** In this work, we assume that all molecules are possible to make, and all molecules are equally time-consuming and costly to make.

**Test** The test step provides noisy test scores of every molecule. It consists of a ground truth providing true test scores and a noise model adding noise to the true scores. We use binary scores where a molecule was either inactive (0) or active (1) with respect to a target modelled by the ground truth. The score of each molecule is determined by the following ratios between counts of carbon  $n_{\text{carbon}}$ , nitrogen  $n_{\text{nitrogen}}$  and oxygen  $n_{\text{oxygen}}$  atoms

$$5.5 \leq \frac{n_{\text{carbon}}}{n_{\text{oxygen}}} \leq 5.67, \quad 7 \leq \frac{n_{\text{carbon}}}{n_{\text{nitrogen}}} \leq 7.39, \quad 1.18 \leq \frac{n_{\text{oxygen}}}{n_{\text{nitrogen}}} \leq 1.34.$$

If at least two of the counts are non-zero and the conditions of these non-zero counts are fulfilled, a molecule is scored as active, yielding a reward of 1. Otherwise, it is scored as inactive, giving a reward of 0. The noise model flips the score with probability 0.01.

**Analyze** In each analyze step, the QSAR model of the scoring function is retrained using the previous and new test scores. Also, the new test scores are used to update the total reward and the number of plays of each ball in the contextual Zooming algorithm with multiple plays and volatile arms, as described in Section 3.

### 4.2 Selection

In each cycle,  $K = 100$  molecules are selected to be made. All previously selected molecules are removed from the list of selectable molecules. This gives the extreme case of volatile base arms where no arm can be selected twice.

In Section 3 we introduced our approach contextual Zooming with multiple plays and volatile arms. Below, we briefly describe other strategies that we study: greedy selection and decaying-epsilon-greedy selection. In our experiments, we also investigate random sampling, which randomly (without replacement) selects base arms in  $\mathcal{M}^t$ .

**Greedy selection** In each round  $t$ , we have scores  $\mathcal{F}^t$  from the scoring function. Greedy selection selects the  $K$  molecules with the highest scores. Ties are broken arbitrarily.

**Decaying-epsilon-greedy selection** In each round  $t$ , decaying-epsilon-greedy ( $\epsilon$ -greedy in short) selects a random compound with probability  $\epsilon_t$  or the (non-selected) maximum scoring molecule with probability  $1 - \epsilon_t$ . This is done until  $K$  base arms are selected. In each round  $t$ , we have  $\epsilon_t = \epsilon_{\min} + (\epsilon_{\max} - \epsilon_{\min}) e^{c_{\text{decay}}(t-1)}$ . We use  $c_{\text{decay}} = 0.015$  and  $\epsilon_{\min} = 0.0$ . In the experiments, we have investigated both  $\epsilon_{\max} = 0.6$  and  $\epsilon_{\max} = 0.4$ .

### 4.3 Comparison of selection strategies

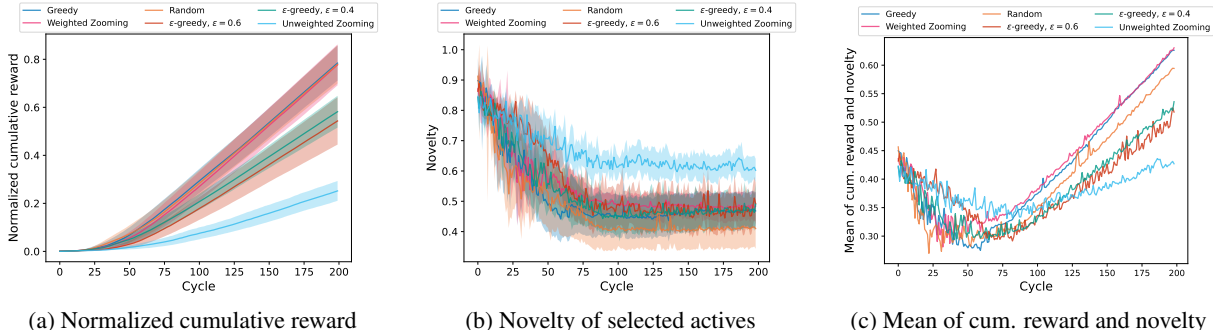


Figure 2: Normalized cumulative reward, novelty of selected actives and the mean of the former two averaged over 10 runs for each selection strategy. For the normalized cumulative reward and novelty, the 95% approximate confidence intervals of the averages over 10 runs is shown.

The normalized cumulative rewards averaged over 10 runs are shown in Figure 2a for various selection strategies. It also shows the 95% approximate confidence interval of the averages over 10 runs for each selection strategy. Weighted Zooming, random sampling and Greedy selection show similar (normalized) cumulative reward after 200 cycles where weighted Zooming is somewhat better. In the last cycles, they show significantly higher cumulative rewards compared to the other strategies. It is reasonable that Greedy selection is able to select active (high rewarding) molecules in the last cycles since then the scoring function has learned sufficient information about the ground truth to guide REINVENT towards generating active molecules. The same is true with random sampling since it is a reflection of the overall activity (reward) of the generated molecules. On the other hand, unweighted Zooming shows lower cumulative rewards compared to the other strategies. An explanation is that more exploration of the chemical space is needed to learn where to identify the most rewarding areas since unweighted Zooming is not inclined toward selecting only actives, as this is the case for weighted Zooming.

Figure 2b shows the novelty of the selected actives averaged over 10 runs for each selection strategy, and the corresponding 95% approximate confidence intervals of each average. Note that no actives are selected in some early cycles of certain runs and, therefore, these runs are excluded when computing the averages and confidence intervals. The novelty at cycle (round)  $t$  is defined as the average dissimilarity to active molecules that have been selected in previous cycles

$$\text{novelty}_t = \sum_{m \in \bigcup_{i=1}^{t-1} \mathcal{A}^i} \frac{1}{|\bigcup_{i=1}^{t-1} \mathcal{A}^i|} \sum_{m' \in \mathcal{A}^t} \frac{\mathcal{D}(x_m, x_{m'})}{|\mathcal{A}^t|},$$

where  $\mathcal{D}(\cdot, \cdot)$  is the Jaccard distance and  $\mathcal{A}^t$  is the true actives selected in cycle  $t$ . That is, a novelty of 1 corresponds to selecting actives that are entirely dissimilar to previously selected actives, i.e., a completely novel selection. In the first cycles, all strategies display a high novelty in the selection of actives. The novelties decrease as more cycles are performed, until after around 100 cycles when the average novelties converge to different values. After this point, unweighted Zooming shows significantly higher novelty compared to the other selection strategies. This observation suggests that unweighted Zooming is able to explore different areas of the chemical space more effectively. Weighted Zooming yields the second-best average novelty, while random sampling leads to the lowest average novelty. The fact that random sampling displays the lowest novelty indicates that the overall diversity of the generated molecules is low by this method, and possibly in general.

The mean of normalized cumulative reward and novelty, averaged over 10 runs, is shown in Figure 2c for each strategy (for illustrative purposes, we discard the confidence intervals). These means indicate how the selection strategies handles the trade-off between maximizing the cumulative reward and selecting novel actives. For all selection strategies, the mean decreases in the beginning but then starts to increase after around 25 to 75 cycles, depending on the strategy. Decaying-epsilon-greedy with  $\epsilon = 0.6$  and unweighted Zooming yield the largest mean for the first 50 cycles, while weighted Zooming and Greedy demonstrate the largest mean for at least the last 100 cycles. Hence, unweighted

Zooming is a good choice in the early phase of the autonomous drug design, while weighted Zooming is better in the late phase. On the other hand, weighted Zooming still performs better than Greedy in the early cycles. This means that a strategy utilizing the benefits of both unweighted and weighted Zooming could possibly provide a promising way to handle the trade-off in all cycles.

## 5 Conclusions

We have formulated the problem of determining what molecule to make next in an automated drug design process as a stochastic multi-armed bandit problem. To solve this problem, we extended the contextual Zooming algorithm [15] to a setting with multiple plays and volatile arms leading to two variants called weighted Zooming and unweighted Zooming. We compared our methods with random sampling, greedy selection and decaying-epsilon-greedy selection. After 200 cycles of a simulated Design-Make-Test-Analyze cycle, we find that Zooming performs overall best and has the potential to be used in autonomous drug design to handle the trade-off between selecting active (high rewarding) molecules and selecting structurally different but still active molecules.

## Acknowledgements

HGS and MHC are supported by the Wallenberg Artificial Intelligence, Autonomous Systems, and Software Program (WASP), funded by the Knut and Alice Wallenberg Foundation, Sweden.

## References

- [1] T. Blaschke, J. Arús-Pous, H. Chen, C. Margreitter, C. Tyrchan, O. Engkvist, K. Papadopoulos, and A. Patronov. Reinvent 2.0: an ai tool for de novo drug design. *Journal of Chemical Information and Modeling*, 60(12): 5918–5922, 2020.
- [2] L. Chen, J. Xu, and Z. Lu. Contextual combinatorial multi-armed bandits with volatile arms and submodular reward. *Advances in Neural Information Processing Systems*, 31, 2018.
- [3] M. Christensen, L. P. Yunker, F. Adedeji, F. Häse, L. M. Roch, T. Gensch, G. dos Passos Gomes, T. Zepel, M. S. Sigman, A. Aspuru-Guzik, et al. Data-science driven autonomous process optimization. *Communications Chemistry*, 4(1):1–12, 2021.
- [4] C. W. Coley, N. S. Eyke, and K. F. Jensen. Autonomous discovery in the chemical sciences part i: Progress. *Angewandte Chemie International Edition*, 59(51):22858–22893, 2020.
- [5] C. W. Coley, N. S. Eyke, and K. F. Jensen. Autonomous discovery in the chemical sciences part ii: outlook. *Angewandte Chemie International Edition*, 59(52):23414–23436, 2020.
- [6] A. Gaulton, L. J. Bellis, A. P. Bento, J. Chambers, M. Davies, A. Hersey, Y. Light, S. McGlinchey, D. Michalovich, B. Al-Lazikani, et al. ChEMBL: a large-scale bioactivity database for drug discovery. *Nucleic acids research*, 40(D1):D1100–D1107, 2012.
- [7] F. Häse, L. M. Roch, and A. Aspuru-Guzik. Next-generation experimentation with self-driving laboratories. *Trends in Chemistry*, 1(3):282–291, 2019.
- [8] J. P. Hughes, S. Rees, S. B. Kalindjian, and K. L. Philpott. Principles of early drug discovery. *British journal of pharmacology*, 162(6):1239–1249, 2011.
- [9] G. Landrum. Rdkit: Open-source cheminformatics, 2006. URL <http://www.rdkit.org>.
- [10] M. Matveieva and P. Polishchuk. Benchmarks for interpretation of qsar models. *Journal of cheminformatics*, 13(1):1–20, 2021.
- [11] J. Meyers, B. Fabian, and N. Brown. De novo molecular design and generative models. *Drug Discovery Today*, 26(11):2707–2715, 2021.
- [12] H. L. Morgan. The generation of a unique machine description for chemical structures—a technique developed at chemical abstracts service. *Journal of Chemical Documentation*, 5(2):107–113, 1965.
- [13] A. Nika, S. Elahi, and C. Tekin. Contextual combinatorial volatile multi-armed bandit with adaptive discretization. In *International Conference on Artificial Intelligence and Statistics*, pages 1486–1496. PMLR, 2020.
- [14] J.-L. Reymond. The chemical space project. *Accounts of Chemical Research*, 48(3):722–730, 2015.
- [15] A. Slivkins. Contextual bandits with similarity information. In *Proceedings of the 24th annual Conference On Learning Theory*, pages 679–702. JMLR Workshop and Conference Proceedings, 2011.

- [16] H. S. Stein and J. M. Gregoire. Progress and prospects for accelerating materials science with automated and autonomous workflows. *Chemical Science*, 10(42):9640–9649, 2019.
- [17] O. J. Wouters, M. McKee, and J. Luyten. Estimated research and development investment needed to bring a new medicine to market, 2009-2018. *Jama*, 323(9):844–853, 2020.